The Electrochemical Society Proceedings Series, Pennington, NJ (1993).
6. G. E. Gray, J. Winnick, and P. A. Kohl, in *Proceedings of the 28th Intersociety Energy Conversion Engineering Conference*, Vol. 1, p. 1139 (1993).
7. C. Scordilis-Kelley and R. T. Carlin, *This Journal*, **140**, 1606 (1993).
8. T. L. Riechel and J. S. Wilkes, *ibid.*, **139**, 977 (1992).
9. T. J. Melton, J. Joyce, J. T. Maloy, J. A. Boon, and J. S. Wilkes, *ibid.*, **137**, 3865 (1990).
10. C. Scordilis, J. Fuller, R. T. Carlin, and J. S. Wilkes, *ibid.*, **139**, 694 (1992).
11. J. S. Wilkes, L. A. Levinsky, R. A. Wilson, and C. L. Hussey, *Inorg. Chem.*, **21**, 1263 (1982).
12. M. A. M. Noel, P. C. Trulove, and R. A. Osteryoung, *Anal. Chem.*, **63**, 2892 (1991).
13. S. Sahami and R. A. Osteryoung, *ibid.*, **55**, 1970 (1983).
14. W. M. Hedges, D. Pletcher, and C. Gosden, *This Journal*, **134**, 1334 (1987).
15. Y.-K. Choi, B.-S. Kim, and S.-M. Park, *ibid.*, **140**, 11 (1993).
16. E. Peled, in *Lithium Batteries*, J. P. Gabano, Editor, p. 43, Academic Press, Inc., New York (1983).
17. A. Meitav and E. Peled, *J. Electroanal. Chem.*, **134**, 49 (1982).
18. S. B. Brummer, V. R. Koch, and R. D. Rauh, in *Materials for Advanced Batteries*, D. W. Murphy, J. Broadhead, and B. C. H. Steele, Editors, p. 123, Plenum Press, New York (1980).
19. R. T. Carlin and C. Scordilis-Kelley, Unpublished results.

Stability of Sodium Electrodeposited from a Room Temperature Chloroaluminate Molten Salt

Gary E. Gray,* Paul A. Kohl, and Jack Winnick****

Georgia Institute of Technology, School of Chemical Engineering, Atlanta, Georgia 30332-0100, USA

ABSTRACT

Room temperature molten salts consisting of 1-methyl-3-ethylimidazolium chloride (MEIC) and aluminum chloride ($AlCl_3$) have been examined as possible electrolytes for a room temperature design of the sodium/iron(II) chloride battery. This work examines the conditions required to achieve efficient reduction and oxidation of sodium from a sodium chloride buffered, neutral melt. Two substrates were examined, tungsten and 303 stainless steel, using both cyclic voltammetry and chronopotentiometry. Melts were protonated using a closed electrochemical cell to allow quantification of the effect of dissolved HCl on the efficiency of the sodium couple. A threshold of approximately 6 Torr HCl partial pressure was observed for sodium plating-stripping. Below this threshold, the sodium couple was not observed. The results show that the sodium plating-stripping efficiency increases with increasing current density; however, the efficiency reaches a maximum and is adversely affected by high overpotentials and extended exposure of the sodium to the melt. It appears that some passivation occurs as even a very thin layer of plated sodium exhibits a steady open-circuit voltage over long periods in the melt.

Introduction

The urgent need for a power source for electric cars as well as consumer electronics has stimulated tremendous efforts in the search for new secondary batteries. The main criterion for such a secondary battery is high energy density, hopefully above 200 Wh/kg. Also necessary are low cost, ready availability of materials, cycle life, acceptable temperature range, and safety, among others. There has been a variety of new batteries based on lithium (in some form) as the anode. While lithium is highly desirable on the basis of weight and voltage, there are uncertainties about supply if widespread application in vehicles occurs. Sodium, on the other hand, is almost limitless, and while heavier than lithium, offers a similar thermodynamic potential.

Sodium-based batteries have been studied for decades, mostly in the sodium-sulfur configuration. Recently, a sodium-iron chloride battery was announced,[1] the "Zebra" cell, operating at 2.35 V with an energy density of ≥130 Wh/kg at the C/5 rate. This battery is shown schematically in Fig. 1. In the uncharged state, a steel matrix is used as the anode current collector, while an iron mesh or similar structure acts as the cathode. The electrolyte is actually in two phases: the solid, β″-alumina, sodium ion conductor which interfaces with the liquid sodium; and the liquid molten salt electrolyte which interfaces with the β″-alumina and the cathode. The properties of these electrolytes set the minimum operating temperature of the cell: ~250°C. First, the melting point of the liquid is ~110°C at its eutectic,[2] but the composition of the melt varies during operation such that 175°C is a practical minimum. Second, the conductivity of the β″-alumina is a strong function of temperature; the resistive loss through this solid becomes prohibitive much below 175°C.

There are several reasons that a room temperature version of this battery would be attractive. First is the most obvious, that for most consumer applications, ambient temperature storage and operation is very convenient. Second, at ambient temperature, a solid sodium anode could be used (mp = 93°C), avoiding the need for a solid separator. This, of course, presumes a liquid electrolyte that can exist in contact with the solid sodium, yet remain a sodium-ion conductor. The room temperature electrolyte replaces the liquid sodium anode with a solid sodium anode, retains a similar porous iron/iron(II) chloride cathode, and replaces both the high temperature molten salt electrolyte and the solid β″-alumina electrolyte with a single molten salt electrolyte.

The existence of electrolytes with many of the properties sought is well known.[3,4] For example, the electrochemical window of melts containing an organic cation and chloride anion, mixed with stoichiometric $AlCl_3$ (so-called neutral melts) has been shown to be very large; at the positive limit the tetrachloroaluminate anion is oxidized to chlorine, at the negative limit the organic cation is reduced. The electrochemical window of the molten salt system is shown in Fig. 2.[5] With supra-stoichiometric $AlCl_3$ the melt is "acidic," the anodic limit remains the same and aluminum is formed at the negative limit; with substoichiometric $AlCl_3$ the cathodic limit remains unchanged and the oxidation of chloride to chlorine occurs at the cathodic positive limit.

* Electrochemical Society Student Member.
** Electrochemical Society Active Member.

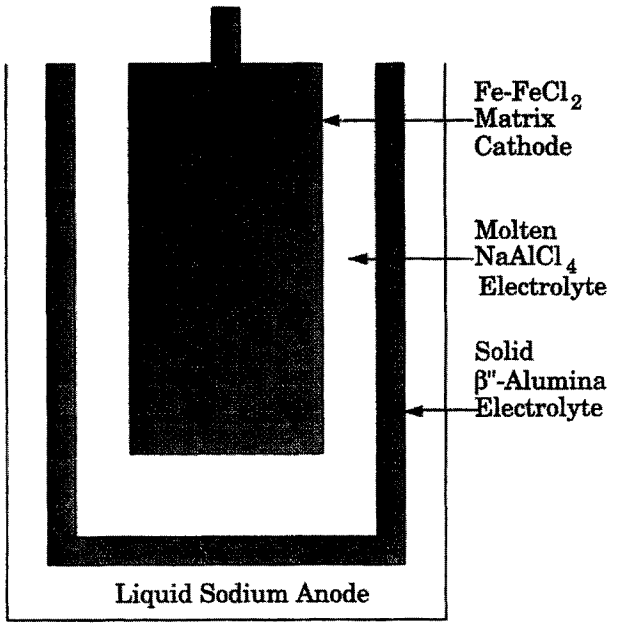

Fig. 1. The high temperature sodium/iron chloride cell.

Thus, the neutral melt is most attractive for the battery application. As with aqueous electrolytes, the method for maintaining a specific acidity is "buffering." In the present case this buffering performs the functions of both maintaining a neutral melt and providing sodium ions. It has been previously shown that sodium chloride can act as a buffer.[6] Sodium chloride reacts with the acidic species ($Al_2Cl_7^-$) to form the neutral species ($AlCl_4^-$) and dissolved sodium. The dissolved sodium maintains neutrality by reacting with any of the basic species (Cl^-) produced in the molten salt. The buffering reactions are shown below

$$NaCl(s) + Al_2Cl_7^- \rightarrow Na^+ + 2AlCl_4^- \quad [1]$$

$$Na^+ + Cl^- \rightarrow NaCl(s) \quad [2]$$

The electrode reactions are

$$\text{Anode: } 2Na \leftrightarrow 2Na^+ + 2e^- \quad [3]$$

$$\text{Cathode: } FeCl_2 + 2e^- \leftrightarrow Fe + 2Cl^- \quad [4]$$

$$\text{Overall: } FeCl_2 + 2Na \leftrightarrow Fe + 2NaCl \quad [5]$$

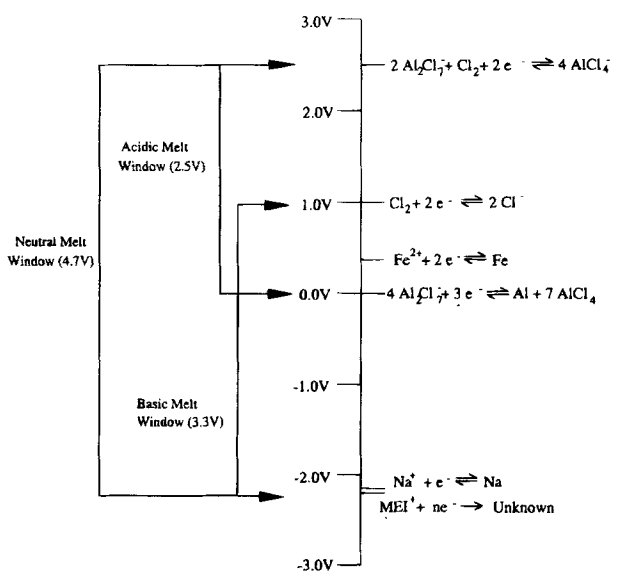

Fig. 2. The electrochemical window of the 1-methyl-3-ethylimidazolium system. Potential of $Fe^{(0)}/Fe^{+2}$ couple approximated from a table of standard reduction potentials.

The first demonstration of the possibility of such a device was by Yu[7] showing that Na could be plated out of this type melt at room temperature. Yu *et al.* plated sodium onto a mercury electrode, thus lowering the activity of the sodium by stabilizing the sodium by the formation of an amalgam. Further work[5] showed that other metal ions (Li and K) could also be reduced at a mercury film electrode. A surprising requirement for the stability of the plated sodium was the presence of protons. This was first demonstrated by Riechel.[3] Scordilis-Kelley and Carlin first reported the reduction of metallic lithium with the addition of protons.[8] Protons can be added to the room temperature molten salt system in the form of gaseous hydrogen chloride.

In this paper, the effect of HCl is quantified using a closed cell. The amount of HCl in the melt was manipulated by adjusting the HCl partial pressure above the molten salt and allowing the system to reach equilibrium. The work has been performed at tungsten and stainless steel because they are of practical value in batteries.

Experimental

All work was performed in a Vacuum Atmospheres dry box with a combined concentration of oxygen and water below 10 ppm. Cyclic voltammetry (CV) and chronoamperometry (CA) were performed with a Princeton Applied Research Model 273 potentiostat/galvanostat interfaced with a personal computer using PAR 270 software. Working electrodes were a 1 mm diam tungsten wire (Alfa 99.98%) sealed in borosilicate glass and a 1.59 mm stainless steel (303) wire sealed in borosilicate glass. Both working electrodes were ground flat to yield a disk of the same diameter as the wire. The counterelectrode was a 1 mm aluminum wire (Fisher ~99.9%) flattened on one end and fashioned into a helix for greater surface area. The reference electrode was a 0.5 mm diam aluminum (Alfa 99.999%) wire inserted into an $N = 0.6$ MEIC/$AlCl_3$ melt in a borosilicate glass tube with an asbestos tip. The electrochemical couple at the reference electrode is between the acidic chloroaluminate species and metallic aluminum

$$4Al_2Cl_7^- + 3e^- \leftrightarrow Al + 7AlCl_4^- \quad E = 0.0 \text{ V}$$

MEIC and $AlCl_3$ were prepared in accordance with previously published procedures.[9] NaCl (Aldrich 99.999%) was heated under vacuum to remove any water present. All buffered, neutral melts were prepared by neutralizing an acidic melt ($N = 0.55$) with double the stoichiometric amount of NaCl needed to reach neutrality. The dissolved sodium concentration was calculated in this way to be 0.95 *M*. The actual concentration of dissolved sodium was not measured. The dissolved sodium was in equilibrium with the excess, undissolved sodium chloride. Although no attempt was made to quantify the kinetics of sodium dissolution, anecdotal evidence suggests it is relatively slow.

A conventional three-electrode cell was used with a bubbler port for the HCl gas. The bubbler was connected to a gas flow system that allowed pure HCl (Matheson, semiconductor grade) or dilute HCl (1% in nitrogen, Matheson) to be mixed with an inert gas (nitrogen or argon, Matheson, UHP). The flow rate of each gas was adjusted using a mass flow controller. The gas mixture was bubbled through the molten salt and out of the system through an oil trap and then neutralized in a sodium hydroxide trap. The cell operated slightly above atmospheric pressure due to the pressure increase across the bubblers. The partial pressure of HCl was calculated assuming ideal gas behavior.

Results

The cathodic stability of the neutral, buffered MEIC-$AlCl_3$-NaCl melt and the effect of melt protonation on the deposition and stripping of sodium were studied. Figure 3A shows a cyclic voltammogram of the unprotonated MEIC-$AlCl_3$-NaCl buffered, neutral melt using a 0.78 mm^2 area tungsten disk. The scan was started at 1.5 V and the initial scan direction was toward negative potentials. The scan rate was 100 mV/s. The cathodic limit of the unprotonated melt was approximately −2.1 V, as defined by the potential

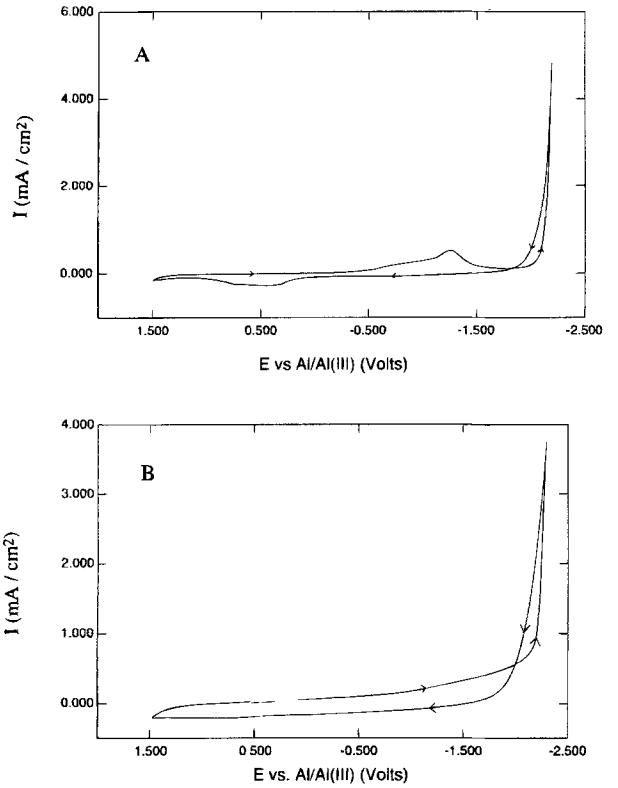

Fig. 3. Cyclic voltammogram of neutral buffered, unprotonated melt at tungsten (A) and 303 stainless steel (B).

at which the electrolyte reduction current was 1.5 mA/cm^3. Riechel and Wilkes attribute the cathodic peak at −1.3 V to the reduction of aluminum.[10] The peak current density for the impurities seen between 1.0 and −1.5 V were greater on a platinum electrode than on a tungsten or stainless steel electrode. This observation is in agreement with that of previous workers.[3] The exact nature of these impurities has not been determined.

It is possible that the cathodic potential range is limited by the reduction of the MEI^+ which may dimerize. It does not appear that Na^+ has been reduced at the negative potential limit on tungsten, because there is no anodic stripping peak observed upon scan reversal at −2.2 V *vs.* the reference. Sodium deposition has previously been observed on a mercury electrode.[5,7] Figure 3B shows a cyclic voltammogram for the buffered neutral melt at a 303 stainless steel disk (2.0 mm^2 area). The scan rate was 100 mV/s. The current peaks at 1.0 V and −1.4 V were much smaller at the stainless steel electrode than at tungsten. The cathodic limit of the melt appears to be the same at 303 stainless steel as with tungsten (*ca.* −2.2 V at 1.5 mA/cm^2).

It has been reported that the addition of protons to the melt extends the cathodic limit of the melt and allows the reduction of Na^+. Gaseous HCl and organic acids have previously been used to protonate the melt.[12] Smith *et al.* formed $MEI^+HCl_2^-$ which is liquid at room temperature by reacting liquid HCl and solid MEIC.[11] Riechel protonated melts by using this liquid proton source. Riechel, Miedler, and Schumacher demonstrated that a shift in reduction potential of the organic cation occurred only in buffered neutral melts.[13] During this study, a similar effect was observed. The potential required to achieve a current density of ~1.3 mA/cm^2 shifted negative approximately 200 mV with HCl addition to the level needed to observe the sodium couple.

The flow cell constructed for this study was used to quantify the effect of protonation with HCl. The partial pressure of HCl was varied by diluting a pure HCl stream with an inert gas (nitrogen or argon). The cyclic voltammogram for the neutral, buffered melt with 5.0 Torr HCl is shown in Fig. 4A. The shift in the cathodic limit of the melt to more negative values can be seen; however, the deposition of sodium was not observed. The current due to the reduction and oxidation of impurities is smaller. The I-V behavior of the neutral, buffered melt with the partial pressure of HCl maintained at 6.1 Torr is shown in Fig. 4B. The sharp rise in the reduction current at approximately −2.3 V again shows the melt is more stable than the unbuffered melt. In Fig. 4B, the cathodic current continues to rise after the sweep reversal at −2.4 V, and a sharp oxidative stripping peak is observed on the positive going scan, which is characteristic of sodium oxidation. The reduction peak is primarily that of sodium reduction. The increase in the reduction current following the scan reversal at −2.4 V can be attributed to the overpotential associated with the nucleation of sodium on tungsten. The kinetic details of this process have not been investigated. Once sodium has been deposited on the surface, the overpotential is reduced and the current rises at the same potential. There is no evidence to suggest the concentration of sodium in at the surface of the electrode is significantly reduced for these experiments using modest currents for short times.

At potentials positive of the sodium redox potential (*ca.* −2.1 V), the electrodeposited sodium is oxidized, resulting in a sharp rise in the anodic current. When the electrodeposited sodium is exhausted, a very sharp drop in the oxidation current is observed. Integration of the reduction and oxidation currents was used to evaluate the coulombic efficiency of the process.

For cyclic voltammetry, the beginning of the reduction process and the end of the oxidation process were chosen based on a significant change in slope of the curve. The end of the reduction process and the beginning of the oxidation process were assumed to occur simultaneously when the current changed from positive to negative. For cyclic voltammetry, the limits of the integration also correspond to the lowest currents. Thus, the technique used in choosing the limits did not result in a significant error in the total charge passed or the calculated efficiency. For chronopotentiometry, the beginning of the reduction process was arbitrarily chosen as the point at which the potential reached −2.0 V. The end the reduction process and the beginning of the oxidation process were asssumed to occur simultaneously when the current was reversed. The end of the oxidation process was chosen based on a significant change in

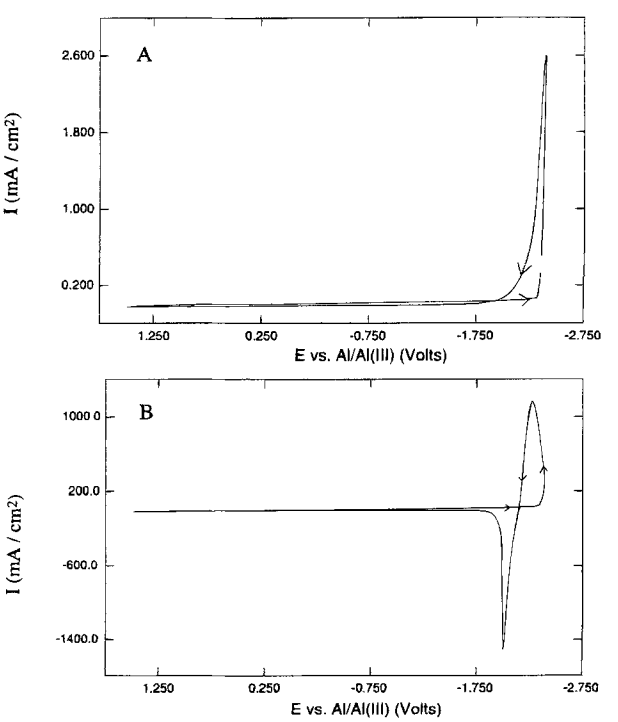

Fig. 4. Cyclic voltammogram at tungsten of a neutral, buffered melt protonated to a partial pressure of: 5 Torr (A) and 6.1 Torr (B) HCl.

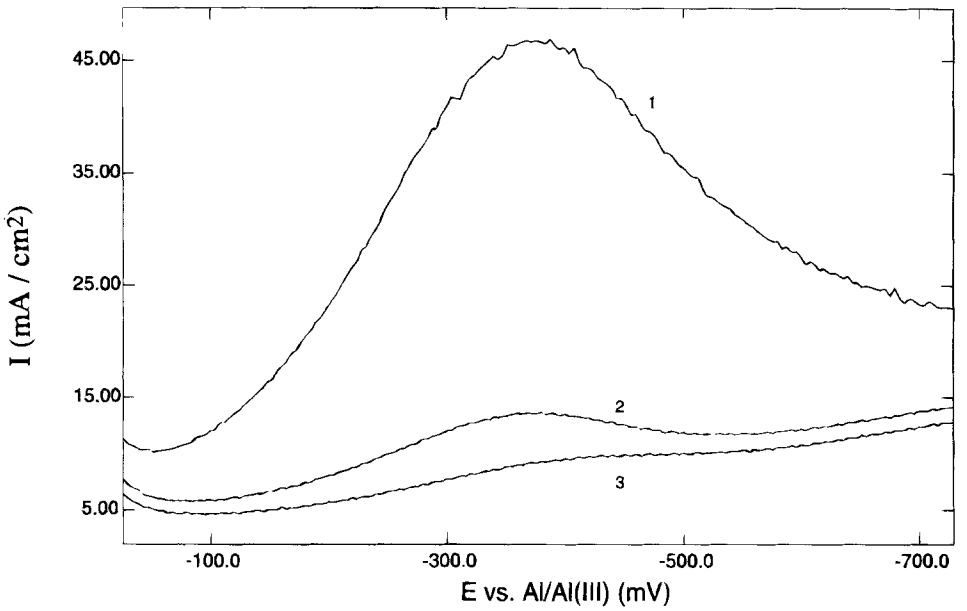

Fig. 5. The reduction peak observed after the addition of protons to the buffered, neutral melt. Initial scan (1) and subsequent scans (2, 3).

slope of the potential *vs.* time curve. For chronopotentiometry, the changes in potential associated with the reduction and oxidation processes were usually very dramatic and the potential changed rapidly with time. Coulombic efficiency is defined as the ratio of oxidation charge associated with sodium stripping divided by the reduction charge associated with sodium plating. The coulombic efficiency for the deposition and stripping of sodium in Fig. 4B is 63%.

The shift in the cathodic stability of the melt with HCl addition is reversible. If the cell is purged with 5 Torr HCl following the 6.1 Torr experiment, no sodium reduction is observed. The cathodic stability shifts back to −2.1 V from −2.3 V when purged with pure nitrogen.

In addition to facilitating the reduction and stripping of sodium, several other I-V effects were observed with the addition of HCl. The impurity peaks observed in Fig. 4 were significantly smaller. A peak attributed to the reduction of protons is shown in Fig. 5 at approximately −0.4 V. The reduction peak decreases with subsequent scans (see scans 1-3) and is seen only following protonation. It can be eliminated by flowing inert gas through the cell and reducing the proton concentration. The reduction of protons has been reported in melts under similar conditions.[14] The diminishing magnitude of this peak with successive scans suggests that it may be due to a surface effect. The peak at −0.4 V is also observed when the melt was protonated with substituted amine • hydrogen chlorides.[12] As the HCl partial pressure was increased, the reduction current associated with the addition of protons also decreased. This unexpected effect was reproducible and was demonstrated in more detail in the chronopotentiometric experiments. It again suggests that this proton-related peak is due to a surface effect, such as changing the chemical composition of an oxide layer on the tungsten surface.

The chemical stability of the sodium in the melt and its coulombic efficiency are very important parameters in the use of this melt and redox couple in a battery application. The coulombic efficiency was investigated as a function of the partial pressure of HCl for the buffered, neutral melt at a tungsten electrode. Figure 6 shows three chronopotentiograms for an unprotonated (Fig. 6A), 5 Torr HCl protonated melt (Fig. 6B), and 6.1 Torr HCl protonated melt (Fig. 6C) at a tungsten electrode. The reduction current was 2.56 mA/cm^2. The oxidative current was the same magnitude after current reversal. The current was reversed after 1 s for the unprotonated melt (Fig. 6A). The proton reduction current at approximately −1.5 V is easily seen, corresponding to the peak seen at −1.5 V in the cyclic voltammogram. Following the consumption of all available reducible species at −1.5 V, a second reduction begins at −2.18 V. After current reversal, the first available oxidation reaction occurs at about 0.6 V. If a reversible sodium couple were present, oxidation of the metallic sodium

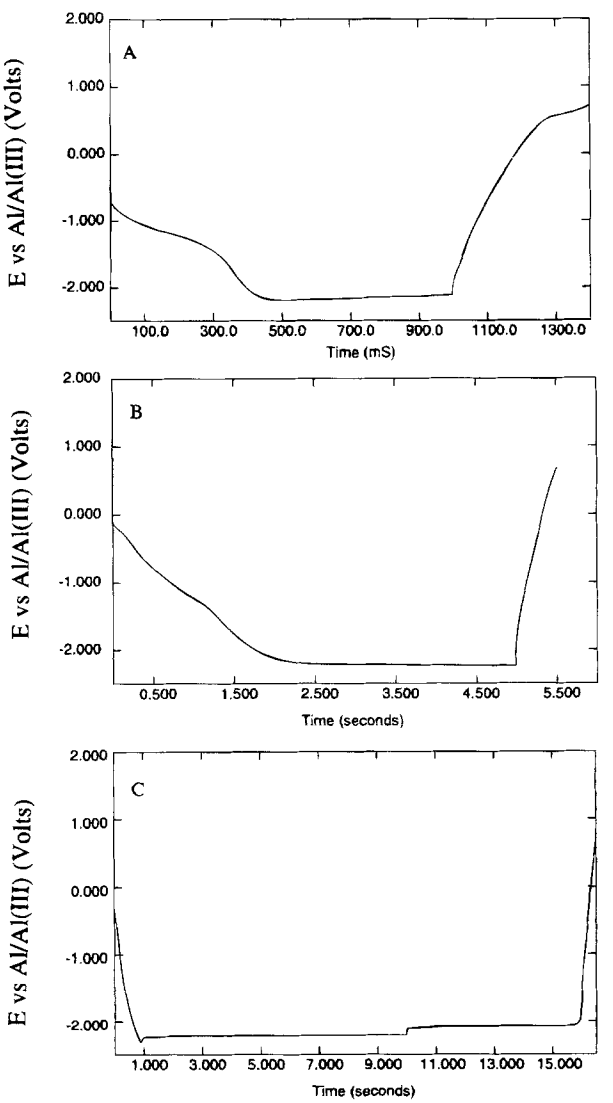

Fig. 6. Chronopotentiograms for the buffered, neutral MEIC/$AlCl_3$/NaCl system with: no HCl added (A), HCl partial pressure of 5 Torr (B), and HCl partial pressure of 6.1 Torr (C).

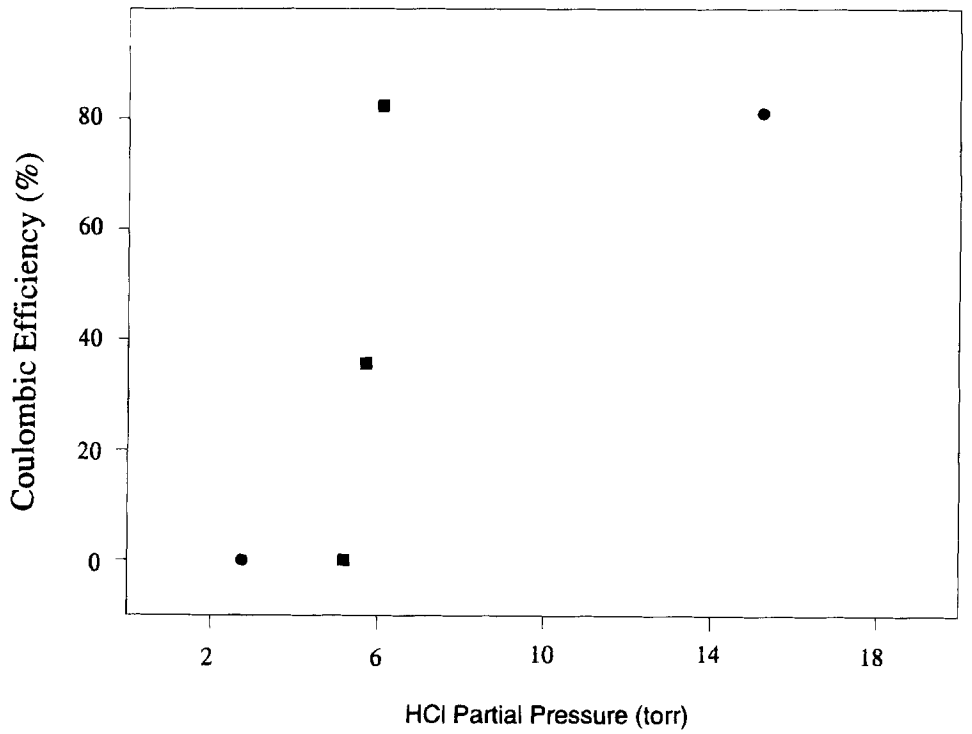

Fig. 7. Coulombic efficiency from cyclic voltammetry (●) and chronopotentiometry (■) *vs.* HCl partial pressure.

would have occurred at approximately −2.1 V. The lack of sodium oxidation shows that the reduction at −2.18 V is either MEI^+ or Na^+ that has already reacted with a melt component.

The effect of 5.0 Torr HCl on the reduction of sodium is shown in Fig. 6B. The increased stability of the melt and proton reduction peak can be seen. No sodium oxidation was observed upon current reversal. The chronopotentiogram of the neutral, basic melt with 6.39 Torr HCl is shown in Fig. 6C. A smaller time for proton-related current is seen, followed by a small overpotential for the nucleation of sodium. Once this initial layer has been deposited, the reduction of additional sodium proceeds at a constant potential of −2.20 V. After current reversal at 10 s, the constant current oxidation of sodium is observed at −2.08 V, followed by the oxidation of the melt beginning at approximately 16 s.

The coulombic efficiency of the sodium couple was measured as a function of HCl partial pressure by both cyclic voltammetry and chronopotentiometry, and is plotted in Fig. 7. The threshold for achieving sodium deposition and stripping is approximately 6 Torr. Below this threshold, no facile sodium couple exists. This threshold effect is reversible. If the HCl partial pressure is decreased below the threshold following protonation of a melt at a partial pressure above the threshold for plating and stripping of sodium, sodium plating is no longer observed. One can repeated purge the melt to a condition above and below the threshold.

The highest coulombic efficiency obtained for the sodium couple was 94%. This maximum efficiency was obtained at tungsten in a constant current experiment at a current density of 6.4 mA/cm^2 and a plating time of 30 s. A series of chronopotentiometric and cyclic voltammetry experiments involving current density, charging time, and current interrupts were performed to help identify the nature of the parasitic reaction.

The effect of current density on the coulombic efficiency of the sodium couple was examined. Using chronopotentiometry, a series of reduction/oxidation experiments were carried out with current densities ranging from ~0.5 to 7 mA/cm^2. The reduction was performed for 60 s followed immediately by oxidation. The effect of current density on efficiency is shown in Fig. 8. These results suggest that for relatively short times and moderate current densities, increasing current density increases the efficiency of the couple to a maximum of about 94%.

Two series of constant charge experiments were performed. First, a set of chronopotentiometric experiments were executed while varying the current density and time of reduction in order to reduce the same amount of sodium (51 mC/cm^2). Immediately after reduction of the sodium at tungsten, the current was reversed and the sodium was oxidized. Current densities ranging from 5 to 25 mA/cm^2 were used. Similarly, current densities ranging from 0.5 to ~13 mA/cm^2 for a total charge of 102 mC/cm^2 were used in a second experiment. It should be noted that at low current densities, the electrodeposited sodium is in contact with the melt for long periods of time, whereas at high current density, the electrode potential is at its most negative value. The results are shown in Fig. 9.

In order to further evaluate the effect of exposure time, an additional series of chronopotentiometric experiments was performed where the reduced sodium was exposed to the melt for nearly a constant time. An open-circuit delay was inserted between the constant current reduction and constant current oxidation so that the time between the start of reduction and the start of oxidation was constant.

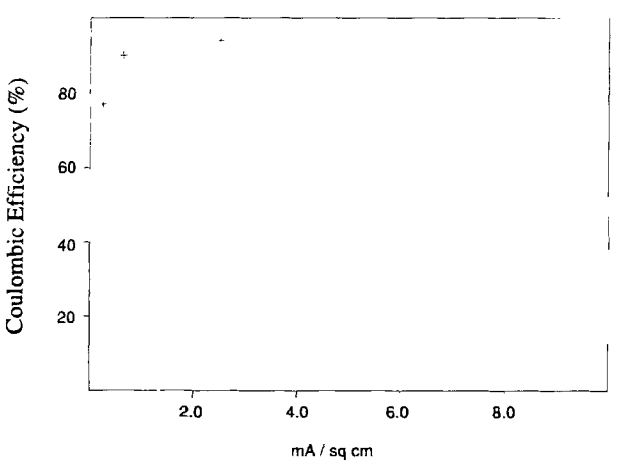

Fig. 8. Coulombic efficiency *vs.* current density for plated sodium on tungsten. The chronopotentiometric reduction was performed for 60 s for all current densities.

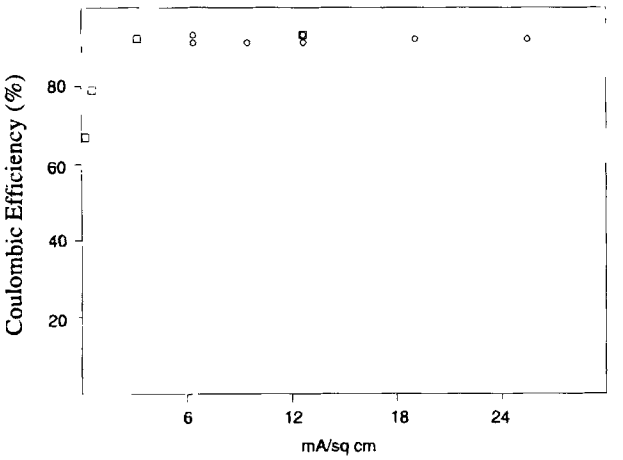

Fig. 9. Coulombic efficiency *vs.* current density for sodium plated on tungsten using chronopotentiometry. The total reduction charge was (□) 51 mC/cm^2 or (○) 102 mC/cm^2.

Current densities ranging from ~0.5 to 5 mA/cm^2 were used. The results of a 1.0 mC reduction using this method at stainless steel are shown in Fig. 10.

Finally, the open-circuit stability of reduced sodium in the buffered neutral melt was studied. Sodium was plated on a tungsten electrode at a current density of 15 mA/cm^2 for 30 s while stirring. This corresponds to 3.6 mC and ~1300 monolayers of electroplated sodium. The open-circuit potential of the electrode was monitored for 3 h at which time the experiment was terminated. The potential of the reduced sodium stayed approximately constant at about −2.1 V with respect to the reference.

Discussion

Examination of the cathodic limit of the buffered, neutral MEIC system with varying levels of protonation shows that HCl extends the reduction limit of the system. There is a threshold partial pressure of HCl which must be reached in order for a facile sodium couple to appear. Riechel's results[3] indicate the concentration of HCl in the melt corresponding to this threshold partial pressure is very low (0.02 mole fraction) compared to the concentration of the organic cation (0.41 mole fraction). Keil showed that HCl combines with free chloride (Cl^-) in melt and that once all the free chloride is consumed, there is marked change in conductivity and HCl partial pressure.[15]

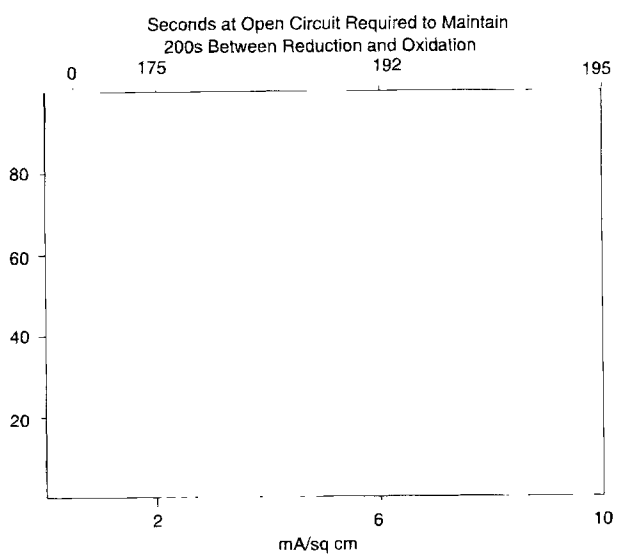

Fig. 10. Coulombic efficiency *vs.* current density for plated sodium on 303 stainless steel. Time between beginning of reduction and beginning of oxidation is constant and the total reduction charge is 51 mC/cm^2.

The low concentration of protons compared to that of other species in the molten salt is inconsistent with the notion that the HCl is causing a Nernstian shift of the reduction potential of all MEI^+ present in the melt. One explanation for the observed shift in the cathodic limit of the melt is that MEI^+ is reduced at slightly different potentials depending on its environment. This leads to the following theory. The reduction of MEI^+Cl^- is slightly positive of the reduction of Na^+ and the reduction of $MEI^+AlCl_4^-$ is slightly negative of the reduction of Na^+. Examination of the equilibrium data for the MEIC/$AlCl_3$ system indicates that in the buffered, neutral state some MEI^+Cl^- does exist in the melt at a very low concentration. The addition of protons to the melt in the form of HCl could titrate the MEI^+Cl^- present to form $MEI^+HCl_2^-$. If the reduction potential for $MEI^+HCl_2^-$ is slightly negative of that for Na^+, then once all the MEI^+Cl^- has reacted, a dramatic shift in the cathodic limit of the melt would be observed and a facile sodium couple could be realized. This theory is consistent with the results shown here and with Riechel's observations if the $MEIHCl_2$ he added to his melts contained excess HCl.

The literature suggests that HCl is not irreversibly bound to MEIC in the $MEIHCl_2$ complex.[14] This is consistent with the observation that the effect caused by proton addition to the MEIC system can be reversed by purging with an inert gas. Additional HCl, above that which is needed to complex MEI^+Cl^- may be observed in portions of the electrochemical window far removed from the cathodic limit. This work shows a reduction process occurring near −0.4 V immediately following protonation. This is consistent with other researchers' findings.[3] This work also shows that a facile sodium couple can exist even when the reduction process near −0.4 V is not present. This observation is explained by the previously stated theory if sufficient protons are present to complex all MEI^+Cl^- available, but no excess HCl is present to be reduced at −0.4 V.

Having established a reasonable explanation for the effect of HCl on the melt, there remains the question of why the sodium couple is less than 100% efficient. Three mechanisms for decreased efficiency have been observed. The first involves reduction processes that occur at potentials positive of the sodium couple. These reactions consume electrons that might otherwise be used for sodium ion reduction. If the species involved in these reactions can diffuse to the electrode surface in sufficient amounts, they can consume current even when the electrode is at the potential for sodium reduction (~2.1 V). If these reactions are reversible, the corresponding oxidations would occur positive of the sodium couple and would result in an apparently inefficient sodium couple. One such reduction is the one observed at −0.4 V and associated with the addition of HCl to the melt. The low coulombic efficiency at lower current densities or long exposure times can easily be seen in Fig. 10.

The second mechanism for decreased efficiency of the sodium couple involves the overpotential at the cathode during sodium reduction. Overpotential due to nucleation of sodium at tungsten has been observed. In protonated melts, the potential for reduction of MEI^+ is shifted slightly negative of the potential for reduction of sodium. Any overpotential for the reduction of sodium can cause the potential of the cathode to shift into the region where reduction of the melt occurs. This additional reduction current is difficult to distinguish from the reduction current associated with sodium reduction and would result in an apparently inefficient sodium couple. This effect has been observed in chronopotentiometric experiments at higher current densities.

The final mechanism for decreased efficiency of the sodium couple is a direct chemical reaction of sodium with the melt components. In this case, sodium is successfully reduced, but before it can be electrochemically oxidized, it reacts chemically with the melt. This results in an inefficient sodium couple. This mechanism is supported by experiments that have an open-circuit delay inserted between reduction and oxidation. Efficiency decreased as open-cir-

cuit time increased. The long open-circuit stability of reduced sodium in contact with the melt suggests that this chemical process proceeds at a slow rate or a rate that diminishes with time. This is perhaps due to a thin, semi-passive film that forms on contact between the sodium and the melt.

Conclusions

Protons, in the form of gaseous HCl, added to buffered, neutral melts of MEIC and $AlCl_3$ have a quantitative effect on the coulombic efficiency of the sodium couple. This effect is only observed after the partial pressure of HCl reaches a threshold of about 6 Torr. This phenomena can be described by three mechanisms. The results suggest all three are occurring and subsequently preventing the formation of a completely efficient sodium couple. These mechanisms are: parasitic reduction of impurities below the sodium reduction potential, coreduction of sodium and of the MEI^+ cation at potentials negative of the sodium couple, and direct chemical reaction of the melt with the electrodeposited sodium. An understanding of these mechanisms is necessary in order to successfully utilize the MEIC/$AlCl_3$ room temperature molten salt system as an electrolyte for the sodium/iron(II) chloride cell.

Acknowledgments

The continuing financial support, cooperation, and technical assistance of the Electric Power Research Institute is gratefully acknowledged. One of us (G.E.G.) acknowledges the support of the Air Force Office Scientific Research through a Laboratory Graduate Fellowship.

Manuscript submitted March 13, 1995; revised manuscript received July 13, 1995.

Georgia Institute of Technology assisted in meeting the publication costs of this article.

REFERENCES

1. R. J. Bones, J. Coetzer, R. C. Galloway, and D. A. Teagle, *This Journal,* **134,** 2379 (1987).
2. J. S. Wilkes, *Room Temperature Molten Salts for Advanced Energy Conversion and Storage,* Frank J. Seiler Research Laboratory, U.S. Air Force Academy, CO.
3. T. L. Riechel and J. S. Wilkes, *This Journal,* **139,** 977 (1992).
4. M. Lipsztajn and R. A. Osteryoung, *Inorg. Chem.,* **24,** 716 (1985).
5. C. Scordilis-Kelley, J. Fuller, R. T. Carlin, and J. S. Wilkes, *This Journal,* **139,** 694 (1992).
6. T. J. Melton, J. Joyce, J. T. Maloy, J. A. Boon, and J. S. Wilkes, *ibid.,* **137,** 3865 (1990).
7. C. L. Yu, J. Winnick, and P. A. Kohl, *ibid.,* **138,** 339 (1991).
8. C. Scordilis-Kelley, J. Fuller, R. T. Carlin, and J. S. Wilkes, *ibid.,* **140,** 1606 (1993).
9. J. S. Wilkes, J. A. Levisky, R. A. Wilson, and C. L. Hussey, *Inorg. Chem.,* **21,** 1263 (1982).
10. T. L. Riechel and J. S. Wilkes, *This Journal,* **140,** 3104 (1993).
11. G. P. Smith, A. S. Dworkin, R. M. Pagni, and S. P. Zingg, *J. Am. Chem. Soc.,* **111,** 525 (1989).
12. B. J. Piersma, in *Ninth International Symposium on Molten Salts,* C. L. Hussey, D. S. Newman, G. Mamantov, and Y. Ito, Editors, PV 94-13, p. 415, The Electrochemical Society Proceedings Series, Pennington, NJ (1994).
13. T. L. Riechel, M. J. Miedler, and E. R. Schumacher, in *Ninth International Symposium on Molten Salts,* C. L. Hussey, D. S. Newman, G. Manantov, and Y. Ito, Editors, PV 94-13, p. 491, The Electrochemical Society Proceedings Series, Pennington, NJ (1994).
14. T. A. Zawodzinski and R. A. Osteryoung, *Inorg. Chem.,* **27,** 4383 (1987).
15. R. G. Keil, An Electrochemical and Spectroscopic Study of Electrode Processes, WRDC-TR-89-2065, Wright Research and Development Center, Wright-Patterson Air Force Base, OH.